

Frequency Regulation in Deregulated Power System Integrated with DFIG and SMES Optimized by TLBO

P. Venkatesh, K. Sri Kumar, K. Sandhya Rani

Abstract: The aim of LFC is to make steady state error to zero and to control the tie line power deviation for each control area. LFC system utilizes basic controllers they are I controller, PI controller, PID controller, cascaded PD-PI controller etc. PID and cascaded PD-PI controllers are proposed for the load frequency regulation problem in two area multi-source power generation system and they are tuned by Teaching and Learning Based Optimization (TLBO) Algorithm. Two area multi-unit systems are considered and every area contains two generating systems; first generating system is a reheat steam turbine and second generating system is a gas turbine. To advance the LFC concert, combinations of Super conducting Magnetic Energy Source (SMES) with and without Doubly Fed Induction Generator (DFIG) wind turbine are included in two areas and their parameters are optimized by TLBO. Frequency regulation and tie line power deviation are controlled by objective function that is Integral of Time multiplied Absolute Error (ITAE) technique. For a small load perturbation the efficiency of the proposed system is examined with three different cases, they are unilateral, bilateral and contract violation cases. The resulting power system is simulated and analyzed using MATLAB Simulink software.

Index terms: cascaded PD-PI controller, DFIG wind turbine, frequency error, frequency regulation, ITAE, proportional integral and derivative (PID) controller, SMES, TLBO Algorithm, tie line power deviation.

I. INTRODUCTION

The detailed theory of LFC has been explained in [1]-[2]. After restructuring of power system, generation systems, transmission systems, distribution systems and independent system operators are established and they need to provide generation-load balance and satisfy total demand and must be operated stably under more competitive environment [3]. Several heuristic methods were presented about LFC in a deregulated environment by many authors [4]-[7]. The power demand on the distribution system seeking from the generation under the control of ISO, the concept of distribution participation matrix (DPM) factors are explained in [8].

Revised Manuscript Received on June 01, 2019.

P. Venkatesh, Electrical and Electronics Engineering, V R Siddhartha Engineering College, Vijayawada, India.

K.Sri Kumar, Electrical and Electronics Engineering, JNTUK, Kakinada, Andhra Pradesh, India

K.Sandhya Rani, Electrical and Electronics Engineering, V R Siddhartha Engineering College, Vijayawada, India.

Intelligent approaches such as Particle swarm optimization (PSO), Firefly and Fruit fly algorithms are worn to tune controller parameters like PI, PID, cascaded PD-PI controllers and fuzzy controller etc.,

These controllers are used to stabilize the system when load is subjected to disturbance under deregulation environment [9]-[10]. The various storage systems of energy are like BESS (Battery Energy Storage Systems), SMES (Super Conducting Magnetic Energy system) etc., helps in providing better response and also it controls the active and reactive power flow in the system for stable operation described in [11]-[12]. Due to huge penetration of wind power into the power system, the frequency of the system may change due to load perturbations. The inertial support and the control in power of the DFIG based wind turbine regulate the frequency for small load disturbances [12]-[14].

For analyzing the deregulated power system LFC issues and performance, the system model consists of two area multi unit thermal-gas deregulated power system. In this two area model, DFIG based wind turbine and SMES units are placed in both control areas. These devices are used to reduce various LFC issues and to improve the system stability. change in power generation in each generating systems, two areas frequency along with tie-line power deviation for three different cases of a deregulated system is also calculated. Simulation of the LFC system has been carried out by using MATLAB/ Simulink environment with PID and cascaded PD-PI controllers optimized by TLBO algorithm.

II. DEREGULATED POWER SYSTEM

The considered deregulated power system consisting of thermal-gas generation units and they are taken from [4]. Thermal-gas system under deregulation is shown in Fig.1. The signal (ACE) is distributed through generation participation matrix or ACE Participation Matrix (APF) in each control area and it is must be equal to one. A distribution system may demands and contract with any generating system for power transaction through distribution participation matrix [8]. In participation matrix the no. of columns is occupied as a no. of distribution systems and no. of rows is occupied as a no. of generating systems of a deregulated power system. The load demand by distribution system is j from generating system unit is i are known as contract participation factors.

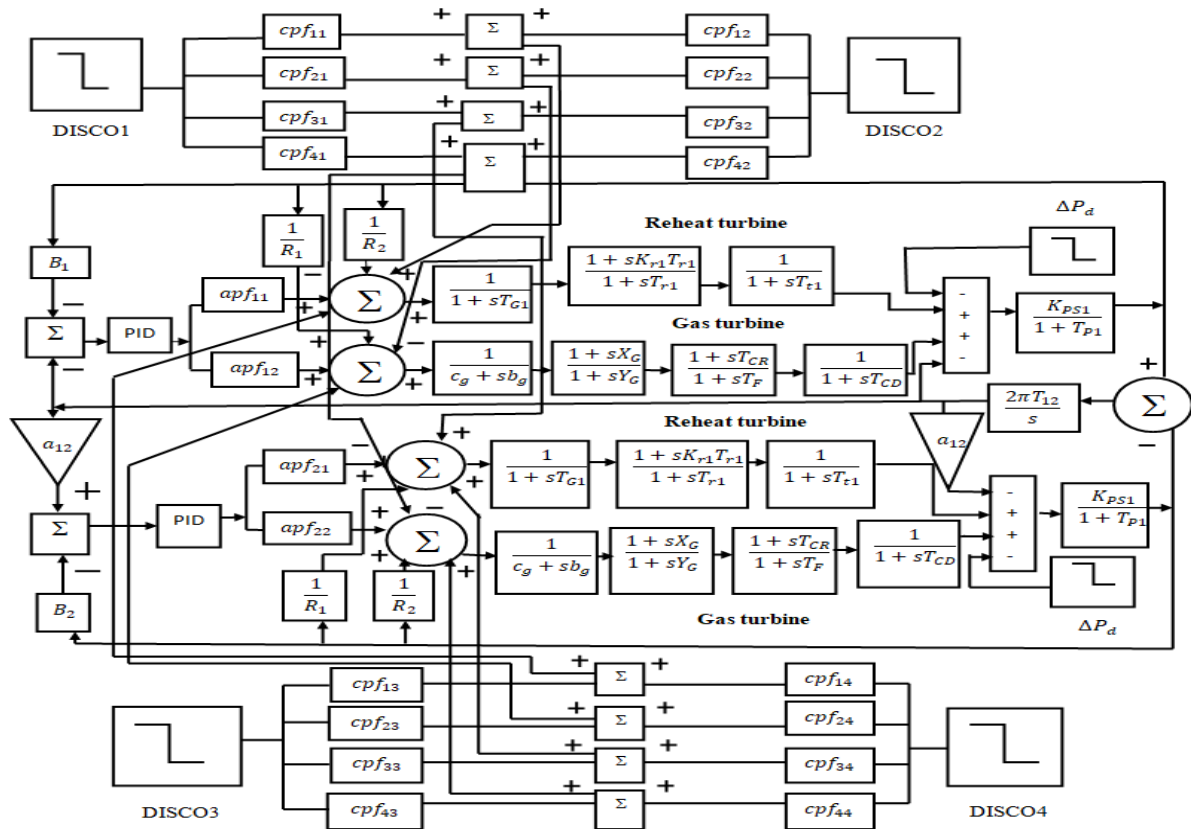


Fig.1. Thermal-Gas system under deregulation.

Tie-line power flow change is given by:

$$\Delta P_{12,scheduled} = (\text{Generation of area-1 to the load demand of area-2}) - (\text{Generation of area-2 to the load demand of in area-1}) \quad (1)$$

Tie line power error change is given by

$$\Delta P_{12,error} = \Delta P_{12,actual} - \Delta P_{12,scheduled} \quad (2)$$

To generate an area control error signal in LFC system tie line power error change is used.

$$e_1(t) = ACE_1 = B_1 \Delta f_1 + \Delta P_{12,error} \quad (3)$$

$$e_2(t) = ACE_2 = B_2 \Delta f_2 + \Delta P_{12,error} \quad (4)$$

$$\Delta P_{21,error} = \alpha_{12} \Delta P_{12,error} \quad (5)$$

Where $\alpha_{12} = \frac{P_{r1}}{P_{r2}}$; P_{r1} and P_{r2} are the rated powers of areas 1 and area 2.

$$ACE_2 = B_2 \Delta f_2 + \alpha_{12} \Delta P_{tie12,error} \quad (6)$$

The Distribution participation matrix of considered two area thermal-gas system is given below.

$$DPM = \begin{bmatrix} cpf_{11} & cpf_{12} & cpf_{13} & cpf_{14} \\ cpf_{21} & cpf_{22} & cpf_{23} & cpf_{24} \\ cpf_{31} & cpf_{32} & cpf_{33} & cpf_{34} \\ cpf_{41} & cpf_{42} & cpf_{43} & cpf_{44} \end{bmatrix} \quad (7)$$

III. DESIGN OF CONTROLLERS

The (PID) controller is the most common and easily understood controller. It improves the system stability and

gives fast response. The modelling of transfer function of PID controller is given below.

$$G_{PID}(S) = K_p + \frac{K_I}{S} + K_D S \quad (8)$$

Cascade control is mostly used to reject the disturbance very fastly [9]-[10]. The input loop is used to attenuate the disturbance. The output loop is used to progress the output quality, the below Fig.2. Shows the configuration of cascaded PD-PI controller.

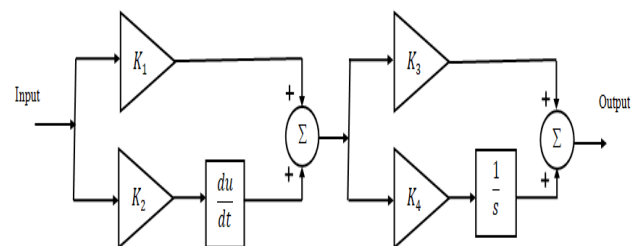


Fig. 2. Configuration of cascaded PD-PI controller.

The objectives function of a considered power system in Eq. (9).

$$J = ITAE = \int_0^{t_{sim}} (\Delta F_1 + \Delta F_2 + \Delta P_{tie}) t dt \quad (9)$$

Where ΔF_1 and ΔF_2 are the frequency deviations, ΔP_{tie} is the tie line power deviation and t_{sim} is the simulation time range.

IV. TLBO ALGORITHM

The TLBO algorithm is a teaching-learning based optimization developed by Rao based on the class room teaching [14]-[15]. The optimization algorithm consisting of two phases they are teacher phase and learner phase. In teacher phase teacher is annoying to improve the knowledge of the learner to give best solution and in learner phase learners of one or more interacting with each other and annoying give the best solution than existing.

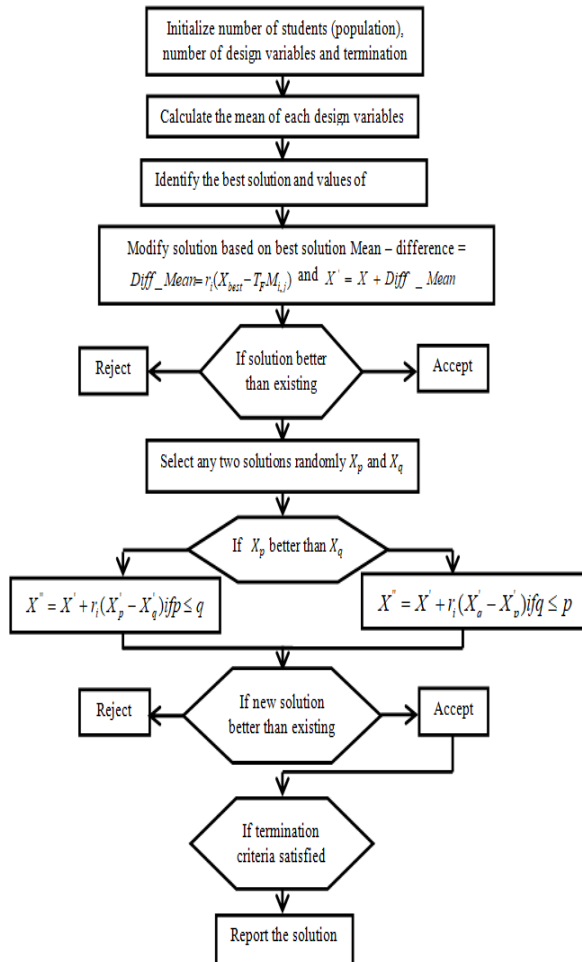


Fig .3. Flow chart of TLBO algorithm.

V. MODELING OF SMES AND DFIG

A. Modeling of SMES

SMES unit is shown in below Fig.4. Coil will be charged to its limit value under normal operation. The inclusion of these devices in SMES is used to regulate the power flows in the system and gives a fast response. Many authors were presented about operation of SMES [11]-[12]. The change in power of superconducting coil is defined as.

$$\Delta P_{SMES} = \left[\frac{1+sT_1}{1+sT_2} \right] \left[\frac{1+sT_3}{1+sT_4} \right] \left[\frac{K_{SMES}}{1+sT_{SMES}} \right] \Delta F_i(s) \quad (10)$$

Where, ΔP_{SMES} is the change in power of magnetic coil, T_{SMES} is the SMES time constant, K_{SMES} is stabilization gain.

The lead-lag compensation block with time constants T_1, T_2, T_3 and T_4 and $\Delta F_i(s)$ is the per unit frequency deviation is used as input signal. The configuration of SMES is shown in Fig.4. These six parameters are to be optimized using TLBO technique.

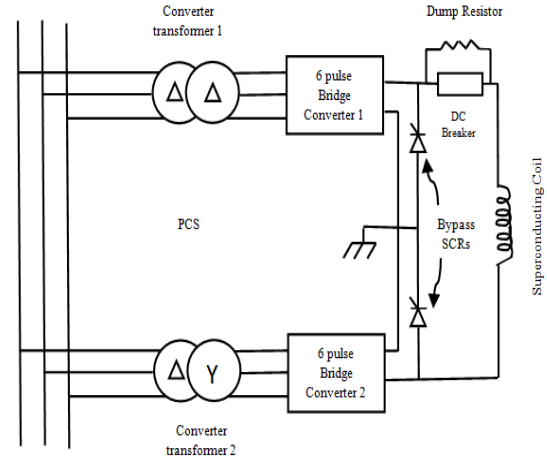


Fig .4. Configuration of SMES unit.

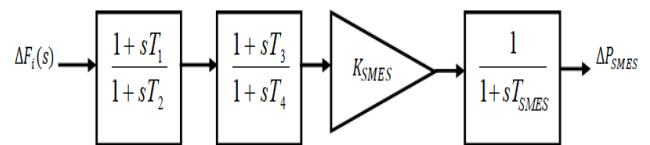


Fig.5. SMES as a frequency stabilizer.

B. Modeling of DFIG

Wind turbine converts electrical energy from the available kinetic energy of wind. power generated by the wind and the input mechanical power extracted by the turbine gives the rotor characteristics of a wind turbine and the operation explained in [12]-[13].

Due to the system inertia, when the frequency droops or rises there is no change in generation by using wind turbine. For analysis of wind turbine inertia emulation model is considered [14]. The basic block diagram of Wind energy control model is shown in Fig.6.

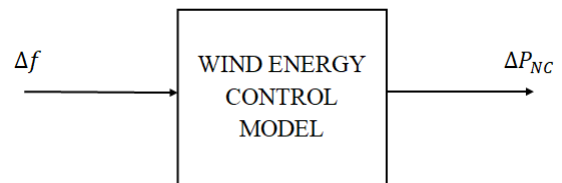


Fig.6. Basic Block diagram of Wind Energy Control Model.

Δf is the change in nominal frequency of the wind energy control system and ΔP_{NC} is the change in non-conventional power.

The speed controller has two inputs, one input from the change in power reference (ΔP_w^*) depending on the electrical power and speed and Second input is from the

change in speed droop (ΔP_f^*) which depends on change in grid system frequency.

$$\Delta P_w^* = K_{wp}(\Delta\omega^* - \Delta\omega) + K_{wi} \int (\Delta\omega^* - \Delta\omega)dt + K_{wd} \frac{d(\Delta\omega^* - \Delta\omega)}{dt} \quad (11)$$

Where K_{wp}, K_{wi}, K_{wd} are the gains of speed controller (PID controller). Configuration of wind energy control model is shown in Fig.7.

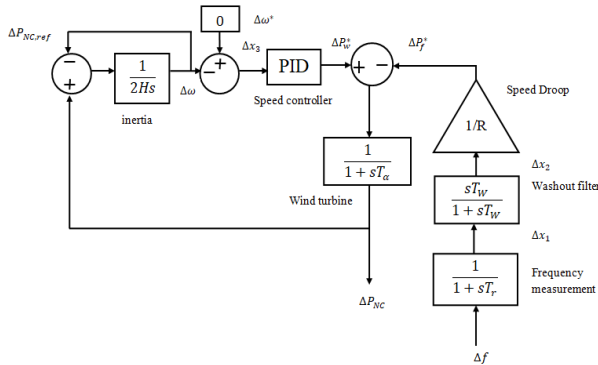


Fig.7. Configuration of Wind Energy Control Model.

The transducer time constant is denoted as T_r and Δx_1 is the change in frequency being measured by transducer used for frequency measurement. The washout filter time constant is denoted as T_w used to smoothen the frequency deviations.

$$\Delta P_f^* = \frac{1}{R} \Delta x_2 \quad (12)$$

Where R is the speed regulation constant value and Δx_2 is the change in grid frequency. $\Delta\omega$ is the change in wind turbine speed and Δx_3 refers to the difference between $\Delta\omega^*$ and $\Delta\omega$.

$\Delta\omega^*$ denotes reference speed which is set to be zero to acquire maximum power output from wind turbine. Speed

controller (PID controller) is used to recover Its optimal speed after completion of transient period and the behaviour of the wind turbine also depends on it.

VI. SIMULATION RESULTS

The considered multi area power system model has two generating systems and two distribution systems. Simulation of frequency regulation of the deregulated power system has been carried out by using the MATLAB/Simulink environment.

A. Unilateral contract

In this case, distribution system and generating system of area 1 both are in contract and the load demanded by distribution system is 10%. The participation factor in every generating system of the considered power system is given below:

Presume that the change in load and the demand occurs only in area 1 by distribution systems of 1 and 2 only. Distribution systems of 3 and 4 are did not contract with generating systems and simultaneous cpfs in participation matrix are zero.

$$DPM = \begin{bmatrix} 0.5 & 0.5 & 0 & 0 \\ 0.5 & 0.5 & 0 & 0 \\ 0 & 0 & 0 & 0 \\ 0 & 0 & 0 & 0 \end{bmatrix}$$

From below figs.8-12 $\Delta f_1, \Delta f_2$ are the parameters of change in frequency responses of both areas and ΔP_{tie} is the change in tie-line power of the system. The time domain specifications of deregulated power system with PID and cascaded PD-PI controllers with combination of SMES-DFIG are optimized by using TLBO algorithm are given in Table I.

Table I. Time domain specifications of unilateral contract case

Responses	Parameters	Unilateral contract			
		PID without DFIG	Cascaded PD-PI without DFIG	PID with DFIG	Cascaded PD-PI with DFIG
ΔF_1	OS	0.075	0.01	0.02	0.004
	US	-0.145	-0.085	-0.095	-0.085
	ST	27.5	5.2	25.4	4.5
ΔF_2	OS	0.025	0.003	0.002	0.001
	US	-0.035	-0.04	-0.017	-0.007
	ST	22.5	10.7	20.6	9.1
ΔP_{tie}	OS	0.0095	0.02	0.002	0.004
	US	-0.074	-0.035	-0.02	-0.0135
	ST	21.8	8.75	18.4	4.95

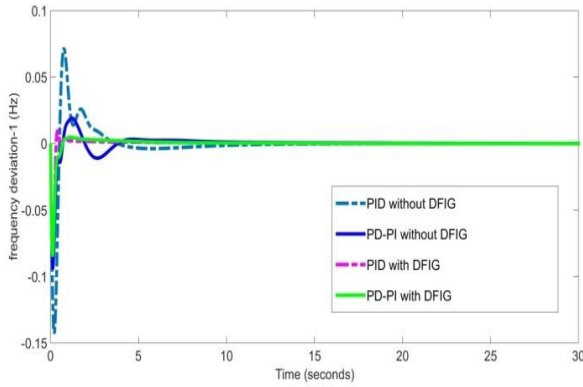


Fig.8. Frequency deviation of area 1 (Δf_1)

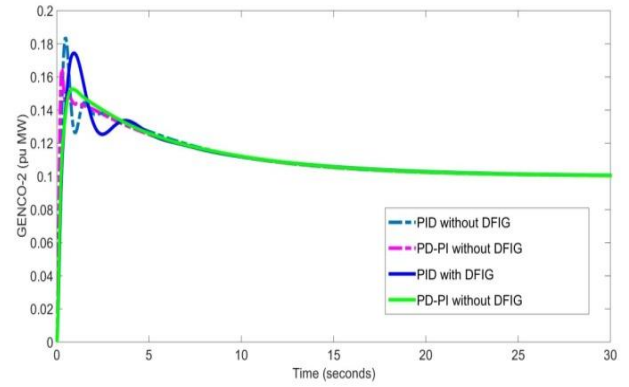


Fig.12. Generation of $GENCO_2 (\Delta P_{G_2})$

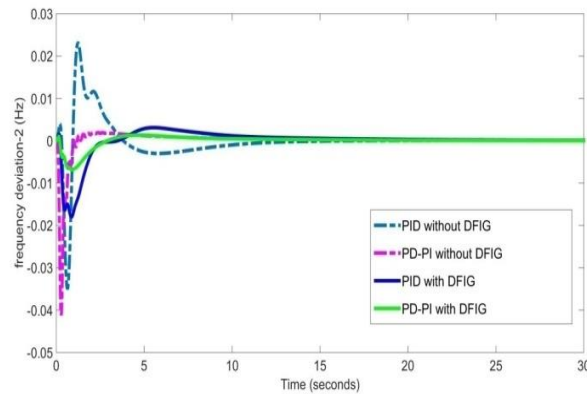


Fig.9. Frequency deviation of area 2 (Δf_2)

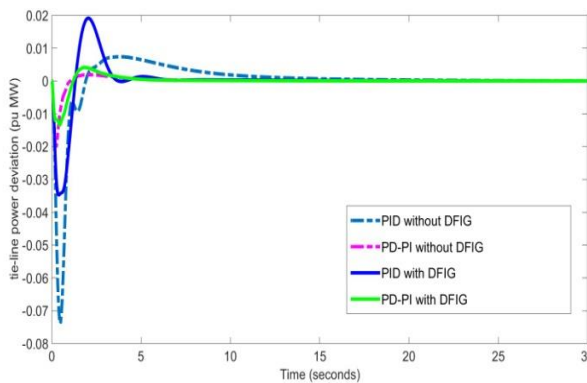


Fig.10. Change in tie-line power (ΔP_{tie})

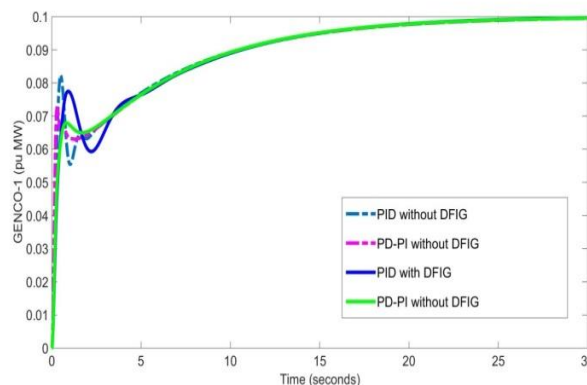


Fig.11. Generation of $GENCO_1 (\Delta P_{G_1})$

In figs.11 and 12, are the parameters of change in generation of the considered system are denoted as ΔP_{G_1} and ΔP_{G_2} for two different controllers with DFIG and without DFIG are shown. From the observation the settling time for cascaded PD-PI controller with and without DFIG is less compared to PID controller. The comparison is shown in Table I.

B. Bilateral contract

In this case, both areas distribution systems are in contract with both areas generating systems for power transaction without any perimeter using below DPM matrix.

$$DPM = \begin{bmatrix} 0.5 & 0.25 & 0 & 0.3 \\ 0.2 & 0.25 & 0 & 0 \\ 0 & 0.25 & 1 & 0.7 \\ 0.3 & 0.25 & 0 & 0 \end{bmatrix}$$

Consider the participation factor in every generating system of the considered power system is given below:
 $apf_1=0.75$; $apf_2=0.25$; $apf_3=apf_4=0.5$

$\Delta f_1, \Delta f_2$ and ΔP_{tie} are shown in below figs.13-19. The comparison is shown in Table II.

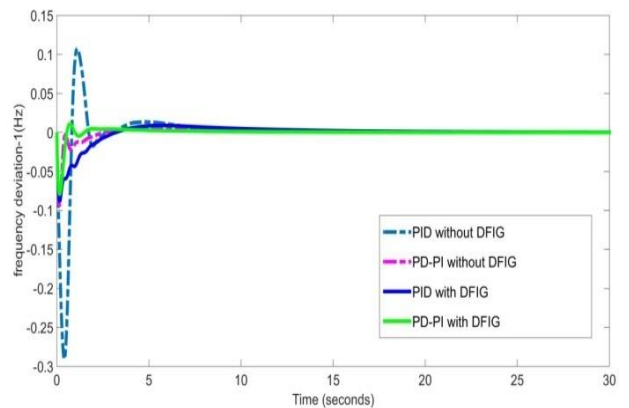


Fig.13. Frequency deviation of area 1 (Δf_1)

Table II. Time domain specifications of bilateral contract case

Responses	Parameters	Bilateral contract			
		PID without DFIG	Cascaded PD-PI without DFIG	PID with DFIG	Cascaded PD-PI with DFIG
ΔF_1	OS	0.11	0.001	0.005	0.001
	US	-0.29	-0.094	-0.0895	-0.0795
	ST	25.5	14.7	24.3	4.95
ΔF_2	OS	0.05	0.002	0.006	0.005
	US	-0.36	-0.148	-0.172	-0.151
	ST	24.8	14.5	20.5	4.75
ΔP_{tie}	OS	0.06	0.01	0.005	0.002
	US	-0.101	-0.05	-0.05	-0.05
	ST	16.7	7.5	14.5	4.35

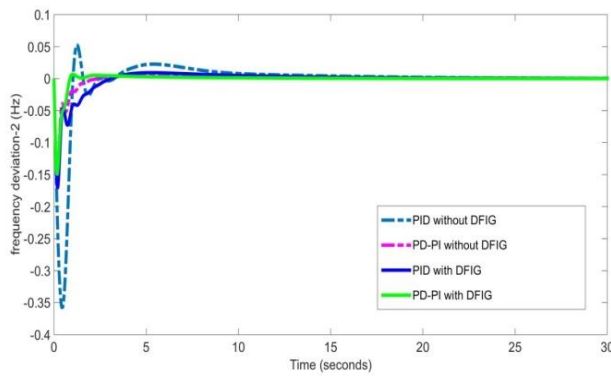


Fig.14. Frequency deviation of area 2 (Δf_2)

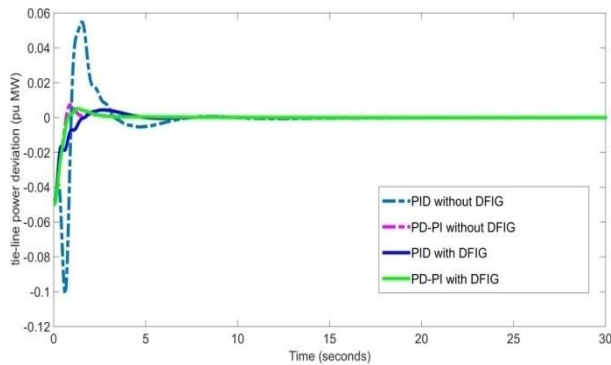


Fig.15. Change in tie-line power (ΔP_{tie})

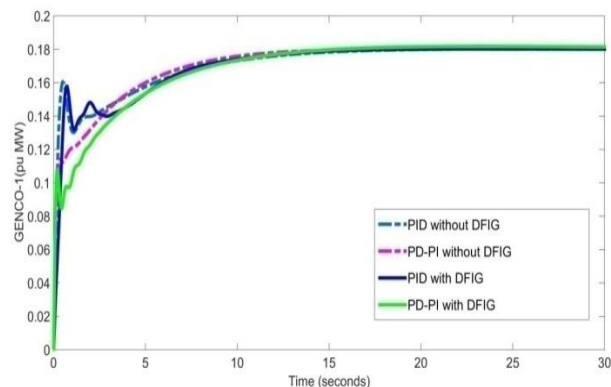


Fig.16. Generation of $GENCO_1(\Delta P_{G1})$

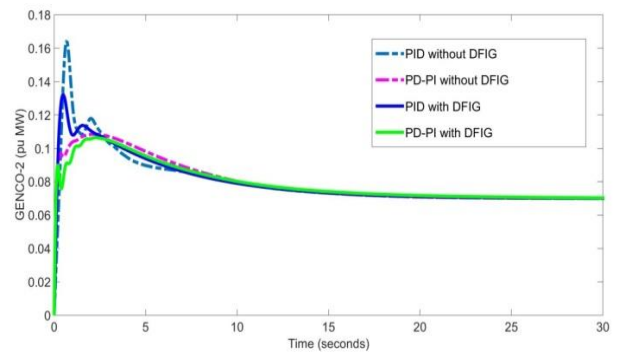


Fig.17. Generation of $GENCO_2(\Delta P_{G2})$

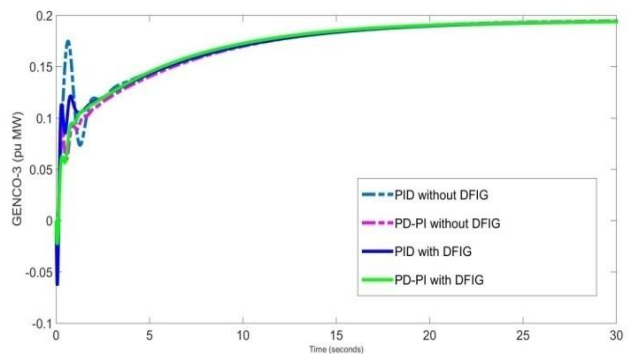


Fig.18. Generation of $GENCO_3(\Delta P_{G3})$

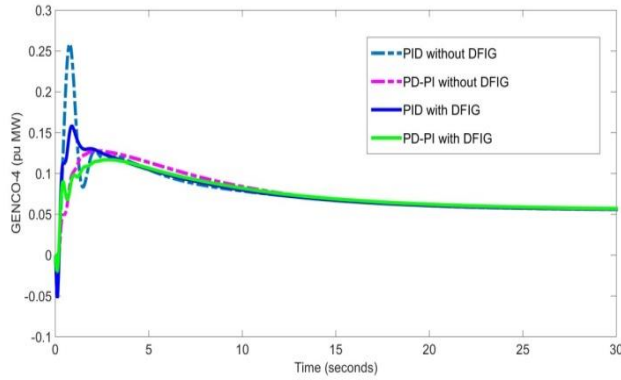


Fig.19. Generation of $GENCO_4(\Delta P_{G4})$

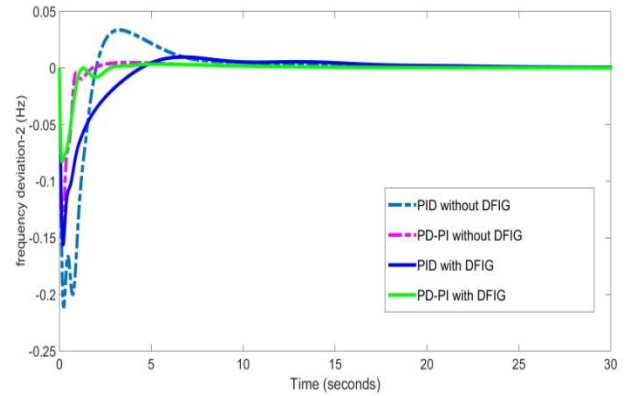


Fig.21. Frequency deviation of area 2 (Δf_2)

In figs.16-19. The change in generation parameters are ΔP_{G1} , ΔP_{G2} , ΔP_{G3} , and ΔP_{G4} of generating systems for two different controllers with and without DFIG optimized by using TLBO algorithm. From observations the settling time for cascaded PD-PI controller is less compared to PID controller.

C. Contract violation

In this case, surplus power demanded by distribution system than essential power is to be supplied by generating system of the same area.

Change in load demand of the area 1 is given below:
 $\Delta P_{L1,loc} = \text{load of } DISCO_1(0.1) + \text{load of } DISCO_2(0.1) + 0.1$
 $= 0.3 \text{ p.u.MW}$

The distribution and generation participation matrix are remains similar to the bilateral contract case. Load demand of area 2 and generation of generating systems 3 and 4 are also remains same as above case. $\Delta f_1, \Delta f_2$ and ΔP_{tie} is the change in tie-line power under contract violation case are shown in below figs.20-26.

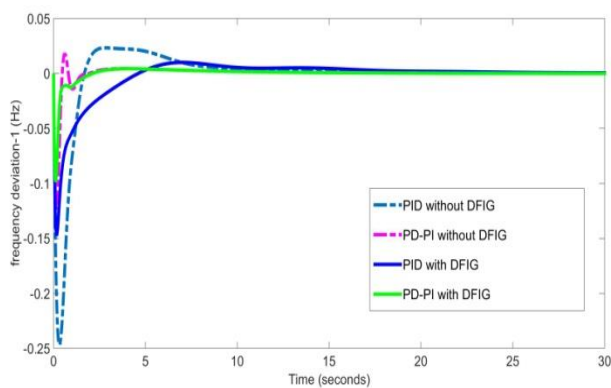


Fig.20. Frequency deviation of area 1 (Δf_1)

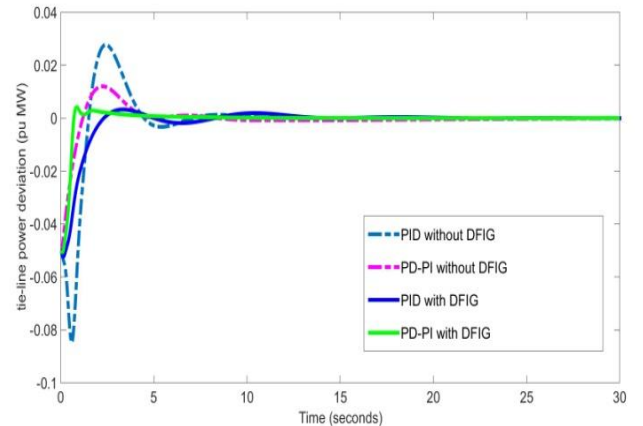


Fig.22. Change in tie-line power (ΔP_{tie})

From observations the settling time for cascaded PD-PI controller is less compared to PID controller is shown in Table III.

Table III. Time domain specifications of contract violations case

Responses	Parameters	Contract violations			
		PID without DFIG	Cascaded PD-PI without DFIG	PID with DFIG	Cascaded PD-PI with DFIG
ΔF_1	OS	0.025	0.02	0.005	0.001
	US	-0.25	-0.121	-0.142	-0.1
	ST	27.3	9.5	26.5	8.5
ΔF_2	OS	0.04	0.005	0.01	0.001
	US	-0.21	-0.149	-0.156	-0.084
	ST	26.4	9.2	25.3	7.4
ΔP_{tie}	OS	0.028	0.012	0.002	0.003
	US	-0.085	-0.05	-0.05	-0.05
	ST	24.5	8.9	20.5	4.9

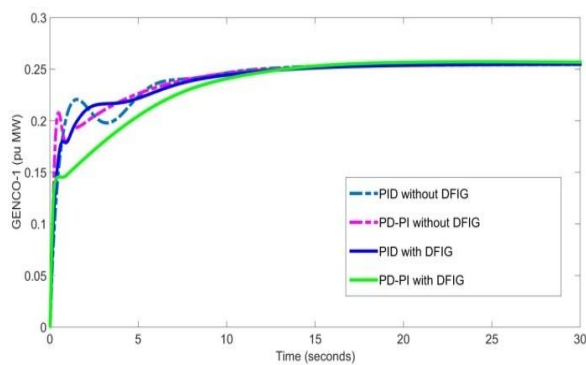


Fig.23. Generation of $GENCO_1(\Delta P_{G1})$

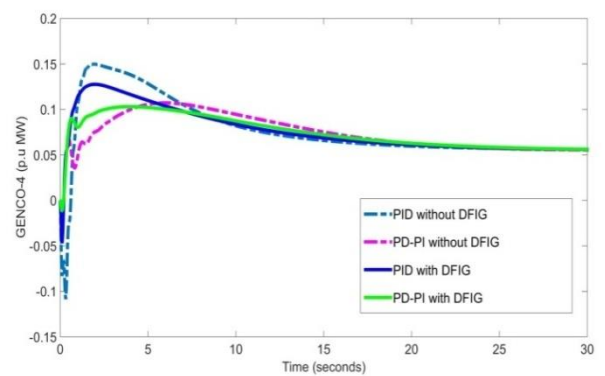


Fig.26. Generation of $GENCO_4(\Delta P_{G4})$

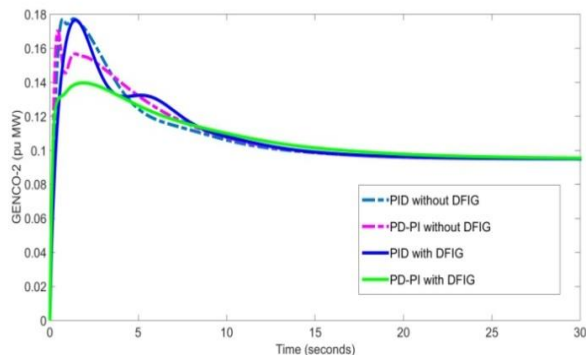


Fig.24. Generation of $GENCO_2(\Delta P_{G2})$

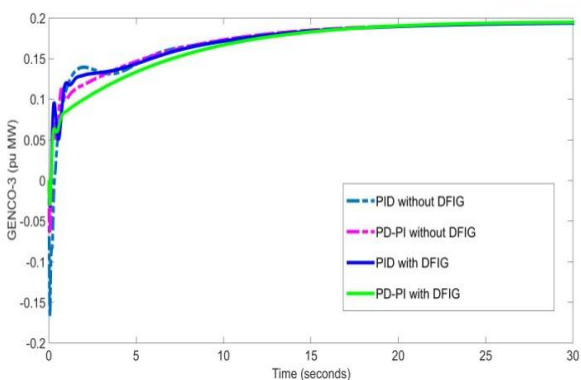


Fig.25. Generation of $GENCO_3(\Delta P_{G3})$

In fig.23-26. The change in generation parameters are $\Delta P_{G1}, \Delta P_{G2}, \Delta P_{G3}$ and ΔP_{G4} of generating systems for two different controllers optimized by using TLBO algorithm.

VII. CONCLUSION

Frequency regulation of two area multi-unit system under deregulated power system with Thermal-gas generation units are considered in each area and SMES-DFIG combination is also used with PID and cascaded PD-PI controllers and these are optimized by TLBO algorithm. Time domain specifications for three different deregulated scenarios are compared. From the simulation results, it is observed that the performance of cascaded PD-PI controller with DFIG gives better results than PID controller without DFIG.

REFERENCES

1. H. Saadat, "Power System Analysis." Tata Mc Graw-Hill: New York, 1999.
2. Kothari.D.Pand Nagrath.U, "Modern power system analysis." Tata McGraw-Hill, (2003).
3. Christie .R.D and Bose.R, "Load frequency control issues in power system operations after deregulation." IEEE Trans Power Syst 11(3),(1996), 1191–200.
4. Hota.P.K,Mohanty, "Automatic generation control of multi source power generation under deregulated

- environment.” *Electrical Power and Energy Systems* 75, 2016, 205–214.
5. Abhijith, Peer Fathima.A, “Load frequency control in deregulated power system integrated with SMES–TCPS combination using ANFIS controller.” *Electrical Power and Energy Systems* 82 ,2016, 519–534.
 6. Barisal.A.K,“Comparative performance analysis of teaching learning based optimization for automatic load frequency control of multi-source power systems.” *Electrical Power and Energy Systems* 66, 2015, 67–77.
 7. Sanjoy. D, Lalit Chandra. S and Nidul.S,“AGC of a multi-area thermal system under deregulated environment using a non-integer controller.” *Electric Power Systems Research* 95, 2013, 175–183.
 8. Donde. V, Pai. M.A, “Simulation and optimization in an AGC system after deregulation.” *IEEE Trans Power Syst* 16(3), 2001, 481–8.
 9. Puja. D, Lalit Chandra. S and Nidul.S,“Automatic generation control of multi area thermal system using Bat algorithm optimized PD–PID cascade controller.” *Electrical Power and Energy Systems* 68,2015, 364–372.
 10. Sidhartha Panda,Patidar. P,Mohan Kolhe,“Cascaded PD-PI Controller for Active Power Frequency Control of Two-Area Multi-Units Power System.” *IEEE International Conference on Power and Renewable Energy*, 2016, pp.251-254.
 11. Nandi.M, Shiva.C.K, Mukherjee.V,“Frequency stabilization of multi-area multi-source interconnected power system using TCSC and SMES mechanism.” *Journal of Energy Storage*, 2017.
 12. Praghmesh.B, Ghoshalb.S.P,and Ranjit Royc, “Coordinated control of TCPS and SMES for frequency regulation of interconnected restructured power systems with dynamic participation from DFIG based wind farm.” *Renewable Energy* 40, 2012, 40-50.
 13. Verma.Y.P and Kumar.A,“Load frequency control in deregulated power system with wind integrated system using fuzzy controller.” *Front. Energy* 7(2), 2013, 245–254.
 14. Verma.Y.P and Kumar.A, “Dynamic contribution of variable-speed wind energy conversion system in system frequency regulation.” *Frontier in Energy*, 2012, 6(2): 184–192
 15. Venkat Rao.R, “Teaching Learning Based Optimization Algorithm.” Switzerland: Springer International Publishing,2016.
 16. Banaja.M, “TLBO Optimized sliding mode controller for multi-area multi-source nonlinear interconnected AGC system.” *Electrical Power and Energy Systems* 73, 2015, 872–881.